



Quantum backaction and noise interference in asymmetric two-cavity optomechanical systems

Yariv Yanay, Jack C. Sankey, and Aashish A. Clerk

Department of Physics, McGill University, Montreal, Canada H3A 2T8

(Received 11 April 2016; published 8 June 2016)

We study the effect of cavity damping asymmetries on backaction in a “membrane-in-the-middle” optomechanical system, where a mechanical mode modulates the coupling between two photonic modes. We show that when the energy difference between the optical modes dominates (i.e., in the adiabatic limit) this system generically realizes a dissipative optomechanical coupling, with an effective position-dependent photonic damping rate. The resulting quantum noise interference can be used to ground-state cool a mechanical resonator in the unresolved sideband regime. We explicitly demonstrate how quantum noise interference controls linear backaction effects and show that this interference persists even outside the adiabatic limit. For a one-port cavity in the extreme bad cavity limit, the interference allows one to cancel all linear backaction effects. This allows continuous measurements of position-squared, with no stringent constraints on the single-photon optomechanical coupling strength. In contrast, such a complete cancellation is not possible in the good cavity limit. This places strict bounds on the optomechanical coupling required for quantum nondemolition measurements of mechanical energy, even in a one-port device.

DOI: [10.1103/PhysRevA.93.063809](https://doi.org/10.1103/PhysRevA.93.063809)

I. INTRODUCTION

The field of quantum optomechanics has largely focused on a relatively simple system, where photons in a single mode of a resonant cavity interact with the motion of a mechanical resonator. This kind of system has been at the heart of a number of recent experimental breakthroughs, ranging from the near ground-state cooling of a mechanical mode [1–3] to the generation of squeezed light [4,5]. Potentially richer behavior can be realized in a system where a mechanical resonator couples to two optical modes, which are in turn tunnel-coupled to one another [6]. By using the avoided crossing of the optical normal modes, such systems can realize an effective quadratic optomechanical coupling, where the adiabatic cavity normal-mode frequencies have no linear dependence on the mechanical position x , but instead depend on x^2 . Such devices could allow quantum nondemolition (QND) measurement of phonon and photon number [6–8] and can realize novel kinds of optomechanical cooling and squeezing [9–11]. Quadratic couplings were first realized in “membrane-in-the-middle” systems, where a movable membrane is placed between two fixed mirrors of a Fabry-Perot cavity [6,12], and more recently in several other experimental setups [13–16].

A key issue in such systems is the presence of residual linear backaction, that is, the linear coupling of external noise sources to the mechanics through the cavity. Such backaction hinders QND phonon-number detection. As discussed extensively by Miao *et al.* [17], linear backaction persists even though the adiabatic normal-mode frequencies depend on x^2 , because the adiabatic wave functions depend linearly on x . When each cavity normal mode is coupled to an independent dissipative reservoir, the linear noise is proportional to the product of both dissipation rates, suggesting that it could be eliminated if one had a truly single-port cavity.

In this work, we revisit linear backaction effects in quadratic-coupling optomechanics, focusing on the case of a realistic, asymmetric two-port cavity. In general, the two dissipative ports each couple to both photonic normal modes as illustrated in Fig. 1, implying that the two modes see

correlated dissipation and noise. In the adiabatic limit, where the splitting of the photonic modes is much greater than all other energy scales, we show that one obtains an effective dissipative optomechanical coupling [18], where the damping rate of each normal mode depends on x . The resulting quantum noise interference implies that one could ground-state cool a mechanical resonator in the unresolved sideband limit [18]. We also explain in detail how this quantum noise interference persists even outside the adiabatic limit and show how standard approximations, which ignore noise correlations, can give misleading results. Note that a related quantum noise cancellation effect was discussed in Ref. [19], where a two-mode optomechanical system couples to a single optical reservoir.

Turning to measurement physics, we show that the interference-based noise cancellation can only be used to cancel all linear backaction effects in the unresolved sideband limit, where the cavity damping rate is greater than the mechanical frequency. In contrast, one needs to be in the opposite (good cavity) limit to make a QND measurement of mechanical energy [6–8]. As a result, even in an ideal one-port device QND measurement of the mechanical energy that can resolve single-phonon jumps requires a single-photon optomechanical coupling that is larger than the cavity damping rate. More optimistically, the cancellation of linear backaction in single-port system in the bad cavity limit allows one to make a measurement of x^2 ; such nonlinear measurement can lead to nonclassical mechanical states [20,21].

II. MODEL

A. Hamiltonian and coupling to environment

The two-cavity optomechanical system of interest is depicted in Fig. 1. Its Hamiltonian takes the form

$$\hat{H} = \hat{H}_{\text{opt}} + \hat{H}_c + \hat{H}_m + \hat{H}_\gamma + \hat{H}_{\text{int}}. \quad (1)$$

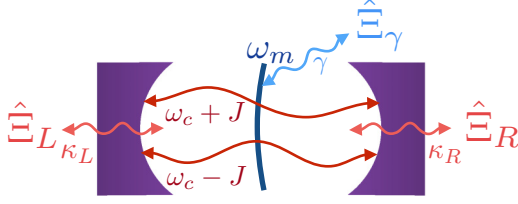


FIG. 1. Schematic of the two-cavity optomechanical system described by Eq. (1). Two cavity normal modes, with energies $\omega_c \pm J$, couple to a moving membrane (frequency ω_m). The optical normal modes are *both* coupled to two independent reservoirs, L and R , with different damping rates, while the membrane is coupled to a third reservoir at damping rate γ .

The Hamiltonian describing the cavities in the absence of optomechanical coupling is ($\hbar = 1$ throughout)

$$\begin{aligned} \hat{H}_{\text{opt}} &= \omega_c(\hat{a}_L^\dagger \hat{a}_L + \hat{a}_R^\dagger \hat{a}_R) - J(\hat{a}_L^\dagger \hat{a}_R + \hat{a}_R^\dagger \hat{a}_L) \\ &= (\omega_c - J)\hat{a}_+^\dagger \hat{a}_+ + (\omega_c + J)\hat{a}_-^\dagger \hat{a}_-, \end{aligned} \quad (2)$$

where \hat{a}_L and \hat{a}_R are the annihilation operators for a pair of localized cavity modes L and R (e.g., to the left and to the right of a membrane at the center of an optical cavity), and J describes a tunnel coupling between them. In the second line, we have diagonalized this Hamiltonian in terms of the optical normal modes $\hat{a}_\pm = \frac{\hat{a}_L \pm \hat{a}_R}{\sqrt{2}}$. The mechanical resonator (frequency ω_m , annihilation operator \hat{b} , position operator \hat{x}) is described by $\hat{H}_m = \omega_m \hat{b}^\dagger \hat{b}$. The optomechanical coupling takes the form $\hat{H}_{\text{int}} = -(\hat{x}/x_{\text{zpt}})\hat{F}_{\text{opt}}$, where

$$\hat{F}_{\text{opt}} = g(\hat{a}_L^\dagger \hat{a}_L - \hat{a}_R^\dagger \hat{a}_R) = g(\hat{a}_+^\dagger \hat{a}_- + \hat{a}_-^\dagger \hat{a}_+) \quad (3)$$

and x_{zpt} is the ground-state position uncertainty of the oscillator. Note that we have scaled the backaction force operator to have units of a rate. In the case of a membrane-in-the-middle type setup, a full derivation of the kind of few-mode description given here is provided in Refs. [7,22]; limitations of the model are discussed in Refs. [22,23].

The remaining terms in Eq. (1) describe dissipation. As is standard, the mechanical dissipation (\hat{H}_γ) is described by a coupling to a thermal Markovian reservoir, giving rise to an amplitude damping rate of $\gamma/2$. The treatment of cavity dissipation (described by \hat{H}_κ) requires slightly more care. We take each of the L and R modes to be coupled to *independent*, zero-temperature Markovian reservoirs. The dissipation of the cavities is thus described by

$$\hat{H}_\kappa = -i(\sqrt{\kappa_L} \hat{\xi}_L^\dagger \hat{a}_L + \sqrt{\kappa_R} \hat{\xi}_R^\dagger \hat{a}_R - \text{H.c.}) + \hat{H}_{\text{ext}}, \quad (4)$$

where $\hat{\xi}_{L,R}$ are bath operators and \hat{H}_{ext} describes the free bath modes. We treat the dissipation as per standard input output theory (see, e.g., Refs. [24,25]). For $J = 0$, the L mode (R mode) has an amplitude damping rate of $\kappa_L/2$ ($\kappa_R/2$). Taking L and R to see independent reservoirs describes the dynamics of a general, asymmetric membrane-in-the-middle type setup [6], where each end mirror of the cavity has a nonzero transmission. We discuss the more general situation, where the two optical eigenmodes are generically coupled to two dissipative reservoirs (e.g., a one port setup with internal loss) in Appendix B.

While Eq. (4) seems innocuous enough, it implies that unless $\kappa_R = \kappa_L$, the optical eigenmodes \hat{a}_\pm will *not* be coupled to independent baths. This implies both that dissipation can couple the two optical normal modes and that their fluctuations are correlated. While it is standard in many quantum optics contexts to ignore such noise correlations between modes that are well-separated in frequency, we show they are significant in this class of systems, as the effects of nonresonant fluctuations are important. Exploring the full consequences of these correlations for a two-cavity system when $\kappa_L \neq \kappa_R$ is the main goal of our work.

B. Heisenberg-Langevin equations

To see this noise correlation explicitly, it is useful to consider the Heisenberg-Langevin equations for our system in the absence of optomechanical coupling. We consider the standard case where the cavity modes are coherently driven at the frequency ω_{dr} near the symmetric normal-mode frequency $\omega_c - J$. Working in a rotating frame at the drive frequency, the optical Hamiltonian takes the form

$$\hat{H}_{\text{opt}} = -\delta \hat{a}_+^\dagger \hat{a}_+ + (2J - \delta) \hat{a}_-^\dagger \hat{a}_-, \quad (5)$$

where $\delta = \omega_{\text{dr}} - (\omega_c - J)$ is the detuning of the driving frequency from the \hat{a}_+ resonance.

By applying standard input-output theory [24,25], the Heisenberg-Langevin equations of motion for our system (at $g = 0$) are easily found. Defining $\bar{\kappa} = \frac{\kappa_L + \kappa_R}{2}$ and $\Delta\kappa = \frac{\kappa_L - \kappa_R}{2}$, we have

$$\begin{aligned} \dot{\hat{a}}_- &= -\left(\frac{\bar{\kappa}}{2} + i\delta - 2iJ\right)\hat{a}_- - \frac{\Delta\kappa}{2}\hat{a}_+ \\ &\quad + \left(\sqrt{\frac{\kappa_L}{2}}\alpha_L^{\text{in}} - \sqrt{\frac{\kappa_R}{2}}\alpha_R^{\text{in}}\right) + \left(\sqrt{\frac{\kappa_L}{2}}\hat{\xi}_L - \sqrt{\frac{\kappa_R}{2}}\hat{\xi}_R\right), \end{aligned} \quad (6)$$

$$\begin{aligned} \dot{\hat{a}}_+ &= -\left(\frac{\bar{\kappa}}{2} + i\delta\right)\hat{a}_+ - \frac{\Delta\kappa}{2}\hat{a}_- \\ &\quad + \left(\sqrt{\frac{\kappa_L}{2}}\alpha_L^{\text{in}} + \sqrt{\frac{\kappa_R}{2}}\alpha_R^{\text{in}}\right) + \left(\sqrt{\frac{\kappa_L}{2}}\hat{\xi}_L + \sqrt{\frac{\kappa_R}{2}}\hat{\xi}_R\right). \end{aligned} \quad (7)$$

We are considering the general case where a coherent cavity drive is applied both at the left port and the right port, with respective classical input field amplitudes α_L^{in} and α_R^{in} . The $\hat{\xi}_i(t)$ operators ($i = L$ and R) describe operator-valued Gaussian white noise, i.e., incident vacuum fluctuations entering the left and right ports. They have zero mean and correlation functions $\langle \hat{\xi}_i^\dagger(t) \hat{\xi}_j(t') \rangle = 0$ and $\langle \hat{\xi}_i(t) \hat{\xi}_j^\dagger(t') \rangle = \delta_{ij} \delta(t - t')$.

One sees clearly that the noise fluctuations driving \hat{a}_+ and \hat{a}_- are in general correlated with one another. These noises are of course identical (and hence completely correlated) in the case of a one-port cavity, $\kappa_R = 0$. The only case where there is no correlation is when $\kappa_R = \kappa_L$. In this case, the situation is identical to having the $+$ and $-$ optical modes coupled to independent reservoirs.

C. Effective dissipative optomechanical coupling

For more intuition into the origin of linear backaction effects in this system, it is useful to consider the structure of the ‘‘adiabatic’’ cavity eigenmodes: if \hat{x} is treated as a static, classical parameter, then what are the cavity eigenmodes for a given value of x ? One finds the lower-energy adiabatic eigenmode is described by

$$\hat{a}_+[x] = \cos[\theta(x)]\hat{a}_L + \sin[\theta(x)]\hat{a}_R, \quad (8)$$

where $\cot 2\theta(x) = gx/Jx_{zpt}$. Its frequency is given by $\omega_+[x] = \omega_c - \sqrt{J^2 + (gx/x_{zpt})^2}$ and depends quadratically on x .

Despite the x^2 dependence of the adiabatic mode frequencies, the dissipation of the adiabatic optical modes can lead to linear backaction. As it couples to the environment through the two leaky mirrors at L and R , the dissipation rate of the + adiabatic mode is

$$\begin{aligned} \kappa_+[x] &= \cos^2[\theta(x)]\kappa_L + \sin^2[\theta(x)]\kappa_R \\ &= \bar{\kappa} + \frac{gx/x_{zpt}}{\sqrt{J^2 + (gx/x_{zpt})^2}} \Delta\kappa. \end{aligned} \quad (9)$$

Unless $\kappa_L = \kappa_R$, the effective damping rate of the adiabatic mode depends on whether the mode is localized more on the left or on the right. As the ‘‘wave function’’ of this adiabatic mode depends on x , one obtains a so-called dissipative optomechanical coupling [18], where the damping rate of an optical mode depends on x . Note that this represents a potentially simpler method for realizing a dissipative optomechanical coupling than the Michelson-Sagnac interferometer proposed in Ref. [26] and realized experimentally in Ref. [27]. We note that recent experiments using trampoline-style resonators in a Fabry-Perot cavity with $\kappa_L \gg \kappa_R$ observed large position-dependent photonic damping [28].

Crucially, to leading order in $1/J$, we see that even though the adiabatic mode frequency has a quadratic dependence on x , $\kappa_+[x]$ depends *linearly* on x for small displacements. This implies that there will be information on x available in the cavity output field, opening the door to unwanted linear backaction effects. It also suggests that the unusual quantum noise physics of a dissipative optomechanical coupling will be relevant here, namely, the possibility of Fano-style interference [17,18].

Note that throughout this discussion we have focused on the lower-energy adiabatic mode, \hat{a}_+ . A full discussion must include the higher-energy adiabatic mode as well, as the two are in general coupled by dissipation. Such coupling effects only contribute at higher orders in $1/J$.

III. BACKACTION QUANTUM NOISE SPECTRUM

We now turn to the question of how noise correlations influence the linear optomechanical backaction on the mechanical resonator. We focus on the standard case where the optomechanical coupling is sufficiently weak that optical backaction effects on the mechanical resonator can be fully understood using linear response theory. This is equivalent to extracting backaction effects from the quantum noise spectrum of the optical force operator \hat{F}_{opt} , evaluated to leading order in g [25,29,30]. We further assume that g is so weak that one

only needs to consider the drive-enhanced optomechanical coupling, i.e., one can linearize the \hat{F}_{opt} operator in the fluctuations of \hat{a}_\pm .

A. Noise spectrum and noise amplitudes

The (unsymmetrized) quantum noise spectral density of \hat{F}_{opt} is defined as [25,29,30]

$$S_{FF}[\omega] = \int dt e^{i\omega t} \langle \hat{F}_{\text{opt}}(t) \hat{F}_{\text{opt}}(0) \rangle. \quad (10)$$

As long as the features of $S_{FF}[\omega]$, such as peaks and dips, are wider than the mechanical linewidth, the cavity can be understood as an effective thermal bath for the mechanics, with an optomechanical damping rate Γ and an effective thermal occupation \bar{n}_{eff} given by

$$\Gamma = S_{FF}[\omega_m] - S_{FF}[-\omega_m], \quad \Gamma \bar{n}_{\text{eff}} = S_{FF}[-\omega_m]. \quad (11)$$

Here, $S_{FF}[+\omega_m]$ describes the emission of energy from the mechanics into the cavity, or cooling processes, while $S_{FF}[-\omega_m]$ describes the absorption of energy by the mechanics, or heating processes.

In our system, the leading terms in \hat{F}_{opt} (which are enhanced by the classical cavity drive) will be linear in the input noise operators. We can thus write it in terms of ‘‘noise amplitudes’’ $\mathcal{A}_{L/R}[\omega]$ as

$$\hat{F}_{\text{opt}}[\omega] = \sum_{i=L,R} \mathcal{A}_i[\omega] \hat{\xi}_i[\omega] + \mathcal{A}_i^*[-\omega] \hat{\xi}_i^\dagger[\omega]. \quad (12)$$

We have defined $\hat{X}[\omega] \equiv \int_{-\infty}^{\infty} e^{i\omega t} \hat{X}(t) dt$ for any operator \hat{X} (implying $\hat{X}^\dagger[\omega] = [\hat{X}[-\omega]]^\dagger$). As the input noise operators describe vacuum noise, one immediately finds

$$S_{FF}[\omega] = |\mathcal{A}_L[\omega]|^2 + |\mathcal{A}_R[\omega]|^2. \quad (13)$$

In addition to controlling the backaction noise spectral density, the noise amplitudes $\mathcal{A}_i[\omega]$ also directly determine how well one can make a linear measurement of position x from the output light leaving the cavities; large linear backaction effects come hand in hand with large amounts of information on x in the output field. This is shown explicitly in Appendix A.

The amplitudes $\mathcal{A}_i[\omega]$ are found by solving the Heisenberg-Langevin Eqs. (6) and (7) in the Fourier domain. They are each a sum of two terms, corresponding to the two optical normal modes \hat{a}_+ and \hat{a}_- :

$$\begin{aligned} \mathcal{A}_{L/R}[\omega] &= \frac{i}{\sqrt{2}} \frac{G}{2\tilde{J}} \sqrt{\kappa_{L/R}} \\ &\times \left[\frac{\varepsilon_m + (i\frac{\Delta\kappa}{2} \mp \Delta J)(1 \pm \frac{\varepsilon_m}{2J})}{\omega + \delta - \Delta J + i\frac{\tilde{\kappa}}{2}} \right. \\ &\quad \left. - \frac{\mp 2J + (i\frac{\Delta\kappa}{2} \pm \Delta J)(1 \pm \frac{\varepsilon_m}{2J})}{\omega + \delta - \Delta J - 2\tilde{J} + i\frac{\tilde{\kappa}}{2}} \right], \end{aligned} \quad (14)$$

where

$$\begin{aligned} G &= g|\langle \hat{a}_+ \rangle|, \quad \frac{\varepsilon_m^*}{2J} = \frac{\langle \hat{a}_- \rangle}{\langle \hat{a}_+ \rangle}, \\ \tilde{J} &= \sqrt{J^2 - \left(\frac{\Delta\kappa}{2}\right)^2}, \quad \Delta J = J - \tilde{J}. \end{aligned} \quad (15)$$

Here, G is the many-photon optomechanical coupling, ε_m is the ratio of the average amplitudes of the optical eigenmodes, and ΔJ is the correction to the eigenmode splitting frequency due to dissipation.

The form of $\mathcal{A}_i[\omega]$ has a simple interpretation: the vacuum noise entering each port of the cavity can contribute to the force noise in two ways, either by exciting the symmetric mode [the first term in the brackets of Eq. (14)], or the anti-symmetric mode [the second term in Eq. (14)]. For small frequencies, the first process is near-resonant, while the second far from resonant. From Eqs. (14) and (13), we see that interference between these two “paths” will in general be important to determining the final value of the noise spectrum. In particular, we have the possibility of using destructive interference to strongly suppress the noise at a given frequency. The fact that interference could play a role in the backaction noise in this system when $\kappa_R = 0$ was briefly mentioned by Miao *et al.* [17]. The interference here is also reminiscent of the backaction cancellation approach used by Caniard *et al.* [31], where two mechanical modes responded to the same fluctuating radiation pressure force.

B. Large- J “adiabatic” limit

We now specialize to the usual situation where the normal-mode splitting J is large, taking $|\omega|, |\delta|, \bar{\kappa} \ll 2J$. The amplitudes determining the force noise then simplify, to leading order in $1/J$, to

$$\mathcal{A}_{L/R}[\omega] = \frac{i}{\sqrt{2}} \frac{G}{2J} \sqrt{\kappa_{L/R}} \left[\frac{-\delta + i\frac{\bar{\kappa}}{2}}{\omega + \delta + i\frac{\bar{\kappa}}{2}} \Lambda^* \mp 1 \right], \quad (16)$$

where $\Lambda = \frac{\sqrt{\kappa_L \alpha_L^{\text{in}}} - \sqrt{\kappa_R \alpha_R^{\text{in}}}}{\sqrt{\kappa_L \alpha_L^{\text{in}}} + \sqrt{\kappa_R \alpha_R^{\text{in}}}}$.

In this regime, the nonresonant term in each amplitude reduces to a frequency-independent constant. The resulting interference implies that the quantum noise spectral density as a function of ω [as given by Eq. (13)] is the sum of two Fano line shapes [32,33]. In general, Fano line shapes can exhibit perfect destructive interference with a vanishing net amplitude. In our case, this will not be possible for both \mathcal{A}_L and \mathcal{A}_R simultaneously, because of the sign difference in the second term in Eq. (16). Hence, at best interference can be used to cancel the noise coming from one port, at one particular frequency.

The above destructive interference becomes even more explicit when one looks at the spectral density, which to leading order in $1/J$ is

$$S_{FF}[\omega] = \frac{G^2}{4J^2} \bar{\kappa} \times \left[\frac{\kappa_L \kappa_R}{\bar{\kappa}^2} + \frac{\left| \frac{\Delta\kappa}{\bar{\kappa}} (\omega + 2\delta) + \left(\delta + i\frac{\bar{\kappa}}{2} \right) \left(\Lambda - \frac{\Delta\kappa}{\bar{\kappa}} \right) \right|^2}{\left| \omega + \delta + i\frac{\bar{\kappa}}{2} \right|^2} \right]. \quad (17)$$

By setting the drive detuning δ (as well as the relative amplitude of the drives applied to each port) one can suppress the second term at a particular frequency, minimizing the noise at this frequency. This is a direct manifestation of the destructive interference discussed above. In particular, for backaction cooling applications, one could choose to minimize the noise

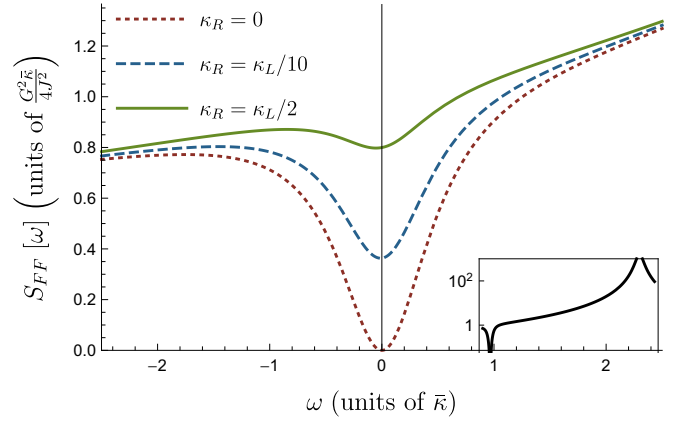


FIG. 2. The spectral noise density $S_{FF}[\omega]$ versus frequency ω , for a two-mode optomechanical cavity driven from the left at the + mode resonance (i.e., $\delta = 0$). We set $J = 10\bar{\kappa}$ to be in the adiabatic regime; curves correspond to different values of κ_R . At $\omega = 0$, the noise density is suppressed as $\kappa_R/\bar{\kappa}$. For $\omega \gtrsim \bar{\kappa}$, the noise density returns to a near-constant value. Inset: $S_{FF}[\omega]$, but now plotted over a wider range of frequencies. One clearly sees two resonances (one near $\omega = 0$, one near $\omega \sim 2J$), corresponding to the two optical normal modes. At this scale all three curves overlap.

at $\omega = -\omega_m$, as this minimizes \bar{n}_{eff} [cf. Eq. (11)]. By using a drive detuning $\delta = \omega_m/2$ and assuming that we only drive the cavity from the L port (i.e., $\alpha_R^{\text{in}} = 0$), we find, to leading order in $1/J$,

$$S_{FF}[-\omega_M] = \frac{G^2}{2J^2} \kappa_R. \quad (18)$$

Equation (18) implies that the “heating” backaction noise vanishes completely in the limit of a one port cavity (i.e., $\kappa_R \rightarrow 0$), so that the cavity backaction acts like a zero-temperature reservoir for the mechanics. This opens the door to ground-state cooling of mechanical resonators that are not in the good cavity limit, something that cannot be done in a standard, coherently driven, single-cavity optomechanical system. We stress that in the large- J limit, this quantum noise cancellation and cooling can be completely understood in terms of the effective dissipative optomechanical coupling in our system (as introduced in Sec. II C).

Shown in Fig. 2 are representative plots of $S_{FF}[\omega]$ which illustrate the noise cancellation effect. The width in frequency of the noise suppression is $\Delta\omega \sim \bar{\kappa}$. This implies that in the extreme bad cavity limit $\omega_m \ll \bar{\kappa}$, one can use this interference to suppress *all* linear backaction effects, i.e., both heating and cooling. In contrast, in the good cavity limit $\omega_m \gtrsim \bar{\kappa}$, it is not possible to use interference to suppress both $S_{FF}[\omega_m]$ and $S_{FF}[-\omega_m]$. As a result, linear backaction effects persist even in a pure single-port system where $\kappa_R = 0$. As we discuss below, this means QND measurement of the phonon number in a one-port cavity of this type is subject to the same tough constraints on the single-photon optomechanical coupling g as in a two-port cavity.

C. Noise interference away from the adiabatic, large- J limit

While the noise spectrum is easiest to understand in the large- J limit, we find that most of the features described

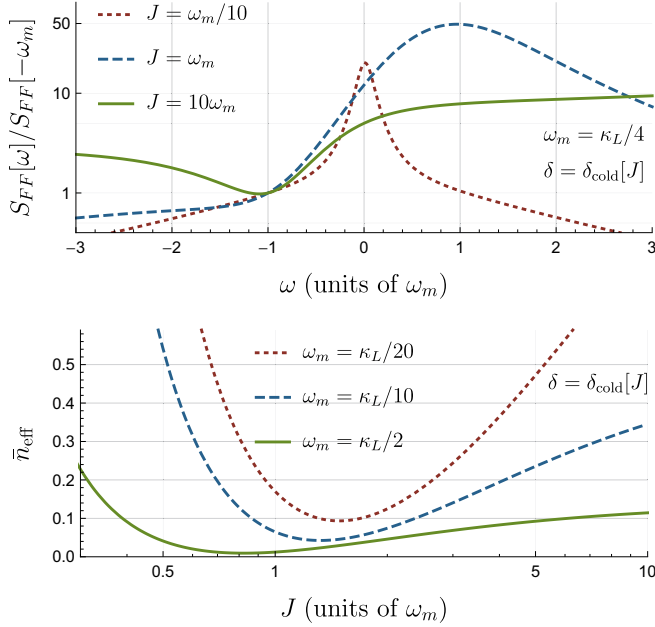


FIG. 3. Behavior of the backaction noise spectral density $S_{FF}[\omega]$ away from the adiabatic, large- J limit. All results correspond to $\kappa_R = \kappa_L/20$ and having set the drive detuning δ to its optimal value for minimizing $S_{FF}[-\omega_m]$: $\delta = \delta_{\text{cold}} = \frac{\omega_m}{2} + J - \sqrt{J^2 + (\frac{\omega_m}{2})^2}$. Top: $S_{FF}[\omega]$ versus ω , for different values of J . All curves correspond to $\omega_m = \frac{\kappa_L}{4}$. We observe the crossover behavior from a Fano line shape to a single peak as J is reduced. Bottom: The effective thermal occupancy \bar{n}_{eff} associated with the cavity backaction as a function of the splitting J of the optical normal modes. It is minimized at the crossover regime $J \sim \omega_m$.

above appear for any value of the mode splitting. Away from the large- J limit, $S_{FF}[\omega]$ does not exhibit a simple Fano resonance, but reflects the interference of the two resonant amplitudes written in Eq. (14). As shown in Fig. 3, one finds a qualitative crossover in the form of the spectrum as J is reduced below $\sim \kappa$ (i.e., when the cavity normal modes are no longer resolved).

Despite the changes in the shape of $S_{FF}[\omega]$, we find that a perfect destructive interference of the noise is possible in the single-port limit for *any* value of J . We stress that, for small J , one is not in the adiabatic limit, and the system is not equivalent to having a dissipative optomechanical coupling.

For $\kappa_R = 0$, the noise spectral density is

$$S_{FF}[\omega] = \frac{2G^2\kappa_L}{(2J - \delta)^2} \left| \frac{J(\omega + 2\delta) - \delta(\omega + \delta)}{2J(\omega + \delta + i\frac{\kappa_L}{4}) - (\omega + \delta)(\omega + \delta + i\frac{\kappa_L}{2})} \right|^2. \quad (19)$$

It can always be made to vanish at $S_{FF}[-\omega_m]$ by setting the detuning $\delta = \frac{\omega_m}{2} + J - \sqrt{J^2 + (\frac{\omega_m}{2})^2} \equiv \delta_{\text{cold}}$. It might seem surprising that the interference persists even for very small values of J , as one would expect to recover the physics of a standard, single-cavity optomechanical system. This is not the case. On the dissipation-free side of the cavity, the average amplitude is inversely proportional J : for $\kappa_R = 0$,

$\langle \hat{a}_R \rangle = \frac{J-\delta}{J} \langle \hat{a}_L \rangle$. As long as there is no loss through the R port, the amplitude in the right cavity can grow arbitrarily large, allowing for perfect destructive interference. The same intuition holds as long as κ_R remains small compared with ω_m and J ; see Sec. V for a more quantitative analysis of this restriction.

For $\kappa_R > 0$, the force noise cannot be made to vanish at any frequency, but the effective thermal occupancy \bar{n}_{eff} associated with the backaction can be minimized by choosing an appropriate drive detuning δ . In general, to achieve a small \bar{n}_{eff} , one would like to both minimize $S_{FF}[-\omega_m]$ (i.e., the ‘‘heating’’ noise), while simultaneously maximizing $S_{FF}[\omega_m]$ (the ‘‘cooling’’ noise). The resonant structure of the noise spectrum has its minimum and maximum near its two poles, which are roughly $2J$ apart [see Eq. (14) and the inset of Fig. 2]. This means that \bar{n}_{eff} is minimized for $J \sim \omega_m$.

IV. CONSEQUENCES FOR QND PHONON MEASUREMENT

A key motivation for the study of membrane-in-the-middle style optomechanical setups is the possibility of QND measurement of mechanical energy eigenstates and the possibility to observe ‘‘quantum jumps’’ in the mechanical energy [6–8,13]. As sketched in Sec. II C (and derived more rigorously in Refs. [6,7]), in the large- J limit one can adiabatically eliminate the off-resonant mode to obtain an effective optomechanical coupling:

$$\hat{H}_{\text{quad}} = -\frac{g^2}{2J} \hat{a}_+^\dagger \hat{a}_+ (\hat{b} + \hat{b}^\dagger)^2. \quad (20)$$

If one further assumes the good cavity limit, the $\hat{b}\hat{b}$ and $\hat{b}^\dagger\hat{b}^\dagger$ terms have negligible influence, leaving only the desired coupling: the frequency of the cavity + mode is controlled by the number of phonons in the mechanical resonator. By driving the + optical mode resonantly (i.e., $\delta = 0$) and making a homodyne measurement of the optical phase quadrature, one can thus monitor the mechanical phonon number.

A. Measurement and backaction time scales

Because of the intrinsic noise in the measured homodyne current, it will take a finite amount of time to resolve the mechanical phonon number. A standard argument [17] shows that the time needed to resolve the mechanical energy to better than one quanta is

$$\tau_{\text{meas}} \sim \frac{J^2\kappa_L}{G^2g^2}. \quad (21)$$

As discussed previously [6,7,17], a successful QND measurement requires that linear backaction effects do not cause a transition of the mechanical state before the measurement can resolve it. For a situation where the mechanical resonator is prepared near its ground state, a minimal requirement is that the measurement time τ_{meas} be shorter than the lifetime of *both* the mechanical ground state and the $n = 1$ Fock state due to backaction. This is illustrated in Fig. 4.

Fermi’s Golden rule lets us directly relate the lifetime of the n th mechanical Fock state to the backaction quantum noise

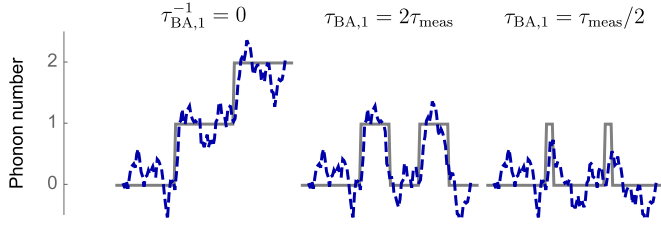


FIG. 4. Illustration of a QND measurement of the phonon number. Plotted as a function of time, the gray lines indicate the behavior of the actual mechanical phonon number, while the dashed blue lines indicate the output signal, averaged over τ_{meas} . At times $t = 4\tau_{meas}$ and $8\tau_{meas}$ the mechanical system experiences an upward quantum jump due to thermal noise unrelated to the cavity. In the absence of backaction ($\tau_{BA,1}^{-1} = 0$), or when the typical backaction is longer than the measurement time ($\tau_{BA,1} = 2\tau_{meas}$), these jumps and the discreteness of the phonon numbers can be observed. When the backaction dominates ($\tau_{BA,1} = \tau_{meas}/2$) the mechanical oscillator appears to remain in the ground state.

spectrum,

$$\tau_{BA,n}^{-1} \equiv (1+n)S_{FF}[-\omega_m] + nS_{FF}[\omega_m]. \quad (22)$$

For driving through the L port at $\delta = 0$ we find

$$\tau_{BA,n}^{-1} = \frac{G^2}{J^2} \left[\frac{\frac{\bar{\kappa}}{2}\omega_m^2 + \kappa_R(\frac{\bar{\kappa}}{2})^2}{\omega_m^2 + (\frac{\bar{\kappa}}{2})^2} + O\left(\frac{1}{J}\right) \right] \left(n + \frac{1}{2} \right). \quad (23)$$

As the mean backaction time decreases with n , the requirement for effective QND measurements is $\tau_{meas}/\tau_{BA,1} < 1$. This ratio is plotted, for a one-port cavity, in Fig. 5.

For a completely symmetric two-port cavity ($\kappa_L = \kappa_R = \bar{\kappa}$), Eq. (23) yields $\tau_{BA,1}^{-1} \sim \frac{G^2}{J^2} \bar{\kappa}$ (with a prefactor ranging from $\frac{1}{2}$ to 1). Combined with Eq. (21), the requirement $\tau_{BA,1} > \tau_{meas}$ for QND measurement then reduces to $g \gtrsim \bar{\kappa}$: the single-photon

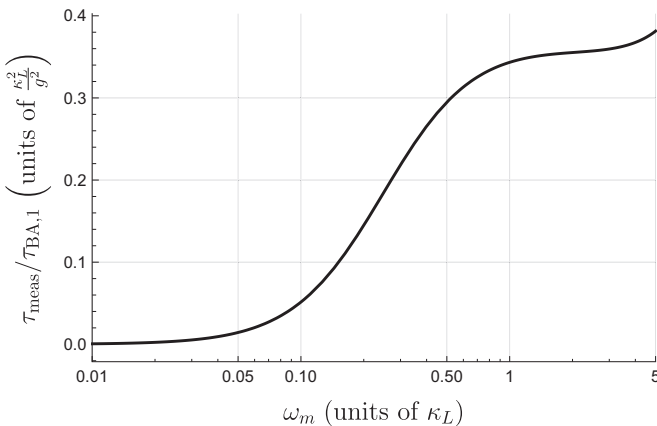


FIG. 5. The relative ratio between typical times for quadratic measurement and for linear backaction, $\tau_{meas}/\tau_{BA,1}$ [see Eqs. (21)–(23)]. As discussed in the text, to perform QND measurements, this ratio must be less than 1. Shown here for a one-port cavity, $\kappa_R = 0$, with $J = 10\kappa_L$ and $\delta = 0$, driving from the left. At $\omega_m \ll \kappa_L$, linear noise is strongly suppressed, while in the good cavity limit its value is similar to the two-port case.

optomechanical coupling rate must be larger than the cavity damping rate. This is in agreement with previous work [17].

For an asymmetric cavity, we must consider separately the resolved and unresolved sideband limits.

B. Resolved sideband limit

To see the discreteness of the mechanical energy, one needs to be in the resolved sideband (i.e., good cavity) limit, $\omega_m \gg \bar{\kappa}$. In this regime \hat{x}^2 is approximately proportional to the phonon number operator, as discussed following Eq. (20). In the resolved sideband limit, Eq. (23) indicates $\tau_{BA,1}^{-1}$ scales as $\frac{G^2}{J^2} \bar{\kappa}$, i.e., in the same way as in the symmetric two-port case. The requirement that $\tau_{BA,1} > \tau_{meas}$ thus reduces again to requiring $g \gtrsim \bar{\kappa}$ for QND measurement. This means that the scale of the optomechanical coupling must be larger than both κ_L and κ_R (and not just their product). A similar conclusion holds in general for a single-sided cavity having internal loss: g must be larger than the coupling κ , not just the internal-loss κ (see Appendix B).

The above conclusion differs from previous works, which suggested that in a perfect one-port cavity, linear backaction effects do not present any limit to performing QND measurement. While it is true that in a single-port cavity, one can perfectly cancel the backaction noise at $\omega = -\omega_m$ via interference [cf. Eq. (17)], the noise at positive frequency $\omega = +\omega_m$ remains. This noise will kill the lifetime of the $n = 1$ Fock state, making it impossible to resolve a quantum jump (see Fig. 4).

Finally, we note that if one manages to achieve a very different situation than that described here, where each optical normal mode couples independently to a separate dissipative reservoir, then one recovers the result of Ref. [17]: the condition $\tau_{BA,1} > \tau_{meas}$ reduces to $g^2 \gtrsim \kappa_+\kappa_-$.

C. Unresolved sideband limit and possibility of x^2 measurement

In the $\omega_m \ll \bar{\kappa}$ limit, we have already shown that noise interference can be used to completely cancel linear backaction effects (see Sec. III B). Thus, not surprisingly, in this limit we find that $\tau_{BA,1}$ diverges as $\kappa_R \rightarrow 0$. In the perfect one-port case, $\kappa_R = 0$, there is no linear backaction at all.

In this limit Eq. (20) does not allow the cavity to measure the phonon number. Instead, the cavity will measure \hat{x}^2 of the mechanics. While such a measurement does not allow one to detect quantum jumps in mechanical energy, its nonlinear nature can allow the conditional generation of highly nonclassical mechanical states, i.e., states which exhibit negativity in their Wigner functions [20,21]. We will explore this physics in detail in a later work.

V. BACKACTION COOLING

In this final section, we return to quantum noise interference that is possible in our system and discuss further the possibilities for mechanical cooling. In the large- J , adiabatic limit, and for $\kappa_R = 0$, the fact that our system allows ground-state cooling of a mechanical resonator in the bad cavity limit is not surprising, as it directly realizes the dissipative $\kappa(x)$ coupling discussed in Ref. [18] (see Sec. II C). More surprising is the

fact that ground-state cooling is possible even away from the large- J limit, where the system is not identical to the dissipative-coupling optomechanical system. As we have seen in Eq. (19) and the surrounding discussion, an effective zero temperature can be achieved for any J given $\kappa_R = 0$.

Driving through the L port, setting $\delta = \delta_{\text{cold}}$ [see Eq. (19) and the following discussion], we find, to leading order in κ_R ,

$$\Gamma = \frac{2G^2}{J^2} \frac{\delta_{\text{cold}}^2}{\omega_m^2 (\bar{n}_{\text{eff}}/\kappa_R)}, \quad (24)$$

$$\bar{n}_{\text{eff}} = \frac{9}{4} \left(\sqrt{1 + \left(\frac{\omega_m}{2J}\right)^2} - \frac{5}{3} \frac{\omega_m}{2J} \right)^2 \frac{\kappa_R}{\kappa_L} + \left(\sqrt{1 + \left(\frac{\omega_m}{2J}\right)^2} - 3 \frac{\omega_m}{2J} \right)^2 \frac{\kappa_L \kappa_R}{16\omega_m^2}. \quad (25)$$

The system can be effectively cooled as long as the internal damping is small enough that $\kappa_L \kappa_R \ll \omega_m^2$. This range of parameters is experimentally realistic [28]. We stress that this small κ_R expansion does not assume anything about the value of J . We also remind the reader that this result is derived within the perturbative, quantum-noise approach. For strong drives, where $\Gamma \sim \bar{\kappa}$, the broadening of the mechanical resonance by Γ leads to an additional nonzero term in \bar{n}_{eff} [34,35].

Finally, note that in the good cavity limit, $\omega_m \gtrsim \kappa_L$, more effective cooling is possible regardless of κ_R by setting the detuning to $\delta \sim -\omega_m$, using the same physics seen in a single-mode cavity [30].

VI. CONCLUSIONS AND OUTLOOK

We have presented a thorough analysis of the residual linear backaction noise in an asymmetric two-mode optomechanical system having the form of the canonical ‘‘membrane-in-the-middle’’ system. Our analysis shows that in the adiabatic, large- J limit, the system has an effective dissipative optomechanical coupling, with a corresponding Fano interference in its quantum backaction noise. Our analysis also shows that this interference (and potential for perfect cancellation) persists even to the nonadiabatic regime for arbitrary J . We demonstrated that in a perfect one-port device in the unresolved sideband regime, all linear backaction effects could be suppressed, allowing an ideal continuous measurement of x^2 . In contrast, if one works in the good cavity limit and attempts to measure quantum jumps in the mechanical phonon number, linear backaction cannot be completely suppressed even in a single-port system, and one requires $g \gtrsim \bar{\kappa}$ for the measurement to be stronger than the unwanted backaction.

We have focused here primarily on a literal membrane in the middle style cavity, but our results hold, qualitatively, for other optomechanical setups where two optical modes are coupled to the mechanics (see Appendix B). The only exception is a system where the two relevant optical normal modes see completely independent dissipation; such systems may be the most promising avenue for the observation of mechanical quantum jumps. An interesting future direction would be to understand how quantum noise interference effects of the sort discussed here manifest themselves in even more complex multimode optomechanical systems.

Note added. Recently, we became aware of a preprint by Khalili *et al.* [36] which also discusses connections between two-mode optomechanical systems and effective dissipative optomechanical couplings.

ACKNOWLEDGMENT

This work was supported by NSERC.

APPENDIX A: CONNECTION TO EFFECTIVE LINEAR MEASUREMENT

We show briefly here that the noise amplitudes $\mathcal{A}_i[\omega]$ introduced in Eq. (12) control how well one could make a measurement of linear position from the output light leaving the cavity. From standard input-output theory, the output field for port $i = L$ and R is given by [25]

$$\hat{a}_i^{\text{out}} = \hat{a}_i^{\text{in}} - \sqrt{\kappa_i} \hat{a}_i. \quad (A1)$$

Using our Heisenberg-Langevin equations, one straightforwardly finds that the fluctuating part of the output field is given by

$$\hat{\xi}_i^{\text{out}}[\omega] = \sum_{j=L,R} \mathcal{B}_{ij}[\omega] \hat{\xi}_j[\omega] - i \mathcal{A}_i[\omega] \hat{x}[\omega]. \quad (A2)$$

Here, the $\mathcal{B}_{ij}[\omega]$ are complex functions of frequency which are independent of the optomechanical coupling g ; they determine the output fluctuations in the absence of any coupling. The second term describes how the output fields depend linearly on \hat{x} ; note that the Heisenberg operator \hat{x} here includes the effects of backaction. We thus see that the linear response kernel linking the output field to $\hat{x}[\omega]$ is identical to the noise amplitudes $\mathcal{A}_i[\omega]$. This result also follows from standard quantum linear response theory (i.e., the Kubo formula), which says that the relevant linear response kernel is given by the commutator of $\hat{\xi}_i^{\text{out}}(t)$ and the backaction force operator $\hat{F}(t)$ (see, e.g., Ref. [25]).

It is illustrative to examine this output in the time domain where we can write

$$\Delta \hat{\xi}_L(t) = \int_{-\infty}^t \mathcal{G}(t-t') \hat{x}(t') dt' \quad (A3)$$

for $\Delta \hat{\xi}_L(t)$, the portion of the output due to coupling to the mechanics. The response function is given by, to first order in $1/J$,

$$\mathcal{G}(\tau) = \frac{G}{2J} \sqrt{\frac{\kappa_L}{2}} \left[\frac{\bar{\kappa}}{2} e^{-\frac{\kappa}{2}\tau} - \delta(\tau - \eta) \right]. \quad (A4)$$

having taken $\Lambda = 1$ and $\delta = 0$. Here, the first terms result from the resonant piece of $\mathcal{A}_L[\omega]$, while the second term comes from the off-resonant piece; η is a positive infinitesimal.

We can see in Eq. (A4) the two regimes described in Sec. IV, caused by the different response rates of the two cavity modes. The response of the rapidly oscillating $-$ mode is near immediate. In the bad cavity regime, when $\omega_m \ll \bar{\kappa}$, the response of the $+$ mode is faster than the rate of change in \hat{x} , leading to a perfect destructive interference. In the good cavity regime, $\omega_m \gg \bar{\kappa}$, the slow response of the $+$ mode means \hat{x} information is averaged out. However, this still leaves the

information leaking through the $-$ mode, which is no longer canceled.

APPENDIX B: GENERIC SETUP

For completeness, we now discuss the generic case, where the cavity is coupled to its environment by some general set of dissipation channels. The damping Hamiltonian of any system coupled to a single driven port and any number of additional

internal loss channels can be written in the form

$$\hat{H}_{\text{damp}} = -i\hat{\Xi}_{\text{dr}}^\dagger(\sqrt{\kappa_{\text{dr}}^+}\hat{a}_+ + \sqrt{\kappa_{\text{dr}}^-}\hat{a}_-) - i\hat{\Xi}_{\text{int}}^\dagger(\sqrt{\kappa_{\text{int}}^+}\hat{a}_+ - \sqrt{\kappa_{\text{int}}^-}\hat{a}_-) + \text{H.c.}, \quad (\text{B1})$$

where $\hat{\Xi}_{\text{dr}}$ and $\hat{\Xi}_{\text{int}}$ are two independent linear combinations of the various dissipation modes, defined so that there is no driving through $\hat{\Xi}_{\text{int}}$. We define here

$$\begin{aligned} \kappa_+ &= \kappa_{\text{dr}}^+ + \kappa_{\text{int}}^+, & \kappa_- &= \kappa_{\text{dr}}^- + \kappa_{\text{int}}^-, & \kappa_{\text{dr}} &= \kappa_{\text{dr}}^+ + \kappa_{\text{dr}}^-, & \kappa_{\text{int}} &= \kappa_{\text{int}}^+ + \kappa_{\text{int}}^-, & \bar{\kappa} &= \frac{\kappa_{\text{dr}} + \kappa_{\text{int}}}{2}, & \delta\kappa &= \frac{\kappa_+ - \kappa_-}{2}, \\ \Delta\kappa &= \sqrt{\kappa_{\text{dr}}^+\kappa_{\text{dr}}^-} - \sqrt{\kappa_{\text{int}}^+\kappa_{\text{int}}^-}. \end{aligned} \quad (\text{B2})$$

At $g = 0$, the equations of motion are

$$\begin{aligned} \dot{\hat{a}}_- &= -\left[\frac{\kappa_-}{2} + i(2J - \delta)\right]\hat{a}_- - \frac{\Delta\kappa}{2}\hat{a}_+ + \sqrt{\kappa_{\text{dr}}^-}(\alpha^{\text{in}} + \hat{\xi}_{\text{dr}}) - \sqrt{\kappa_{\text{int}}^-}\hat{\xi}_{\text{int}}, \\ \dot{\hat{a}}_+ &= -\left(\frac{\kappa_+}{2} - i\delta\right)\hat{a}_+ - \frac{\Delta\kappa}{2}\hat{a}_- + \sqrt{\kappa_{\text{dr}}^+}(\alpha^{\text{in}} + \hat{\xi}_{\text{dr}}) + \sqrt{\kappa_{\text{int}}^+}\hat{\xi}_{\text{int}}, \end{aligned} \quad (\text{B3})$$

and we find

$$\frac{\varepsilon_m^*}{2J} = \frac{\langle \hat{a}_- \rangle}{\langle \hat{a}_+ \rangle} = \frac{\delta + i\frac{\kappa_+}{2} - i\frac{\Delta\kappa}{2}t_d}{-2J + \delta + i\frac{\kappa_-}{2} - i\frac{\Delta\kappa}{2}t_d} t_d \quad (\text{B4})$$

and

$$\begin{aligned} \mathcal{A}_{\text{dr/int}}[\omega] &= \frac{iG}{2\tilde{J}}\sqrt{\kappa_{\text{dr/int}}^+} \times \left[\frac{\varepsilon_m(1 + \frac{i\delta\kappa}{2J}) + i\frac{\Delta\kappa}{2}(1 \pm \frac{\varepsilon_m}{2J}t_d/i) \mp \Delta J(t_d/i \pm \frac{\varepsilon_m}{2J})}{\omega + \delta - \Delta J + i\frac{\kappa_+}{2}} \right. \\ &\quad \left. - \frac{\mp 2Jt_d/i(1 + \frac{i\delta\kappa}{2J}) + i\frac{\Delta\kappa}{2}(1 \pm \frac{\varepsilon_m}{2J}t_d/i) \mp \Delta J(t_d/i \pm \frac{\varepsilon_m}{2J})}{\omega + \delta - \Delta J - 2\tilde{J} + i\frac{\kappa_-}{2}} \right], \end{aligned} \quad (\text{B5})$$

where $t_d/i = \sqrt{\kappa_{\text{dr/int}}^-/\kappa_{\text{dr/int}}^+}$ and here

$$\tilde{J} = \sqrt{\left(J + i\frac{\delta\kappa}{2}\right)^2 - \left(\frac{\Delta\kappa}{2}\right)^2} \quad \Delta J = J + i\frac{\delta\kappa}{2} - \tilde{J}. \quad (\text{B6})$$

For a small internal loss, the noise spectral density becomes, to leading order in $1/J$,

$$S_{\text{FF}} = \frac{G^2}{4J^2} \frac{1}{|\omega + \delta + i\frac{\kappa_+}{2}|^2} \left[\kappa_{\text{dr}}^- |\omega + 2\delta|^2 + \kappa_{\text{int}}^- \left| \omega + \delta \left(1 - \frac{t_d}{t_i}\right) + i\frac{\kappa_+}{2} \left(1 + \frac{t_d}{t_i}\right) \right|^2 \right]. \quad (\text{B7})$$

We see that, while the factors vary, the structure of the force noise and the noise density spectrum are similar to those discussed in the main text and seen in Eqs. (14) and (17).

In particular, for the purpose of QND measurement, a single-port system in the good cavity limit has $\tau_{\text{BA},1} \sim \frac{G^2}{J^2}\kappa_{\text{dr}}^-$, leading to the requirement $g \gtrsim \kappa_{\text{dr}}^-$. Thus, QND measurements are possible when the off-resonant channel is not coupled to the driving port.

- [1] J. D. Teufel, T. Donner, D. Li, J. W. Harlow, M. S. Allman, K. Cicak, A. J. Sirois, J. D. Whittaker, K. W. Lehnert, and R. W. Simmonds, *Nature (London)* **475**, 359 (2011).
- [2] J. Chan, T. P. M. Alegre, A. H. Safavi-Naeini, J. T. Hill, A. Krause, S. Gröblacher, M. Aspelmeyer, and O. Painter, *Nature (London)* **478**, 89 (2011).

- [3] R. W. Peterson, T. P. Purdy, N. S. Kampel, R. W. Andrews, P.-L. Yu, K. W. Lehnert, and C. A. Regal, *Phys. Rev. Lett.* **116**, 063601 (2016).
- [4] D. W. C. Brooks, T. Botter, S. Schreppler, T. P. Purdy, N. Brahms, and D. M. Stamper-Kurn, *Nature (London)* **488**, 476 (2012).
- [5] A. H. Safavi-Naeini, S. Gröblacher, J. T. Hill, J. Chan, M. Aspelmeyer, and O. Painter, *Nature (London)* **500**, 185 (2013).

- [6] J. D. Thompson, B. M. Zwickl, A. M. Jayich, F. Marquardt, S. M. Girvin, and J. G. E. Harris, *Nature (London)* **452**, 72 (2008).
- [7] A. M. Jayich, J. C. Sankey, B. M. Zwickl, C. Yang, J. D. Thompson, S. M. Girvin, A. A. Clerk, F. Marquardt, and J. G. E. Harris, *New J. Phys.* **10**, 095008 (2008).
- [8] M. Ludwig, A. H. Safavi-Naeini, O. Painter, and F. Marquardt, *Phys. Rev. Lett.* **109**, 063601 (2012).
- [9] M. Bhattacharya, H. Uys, and P. Meystre, *Phys. Rev. A* **77**, 033819 (2008).
- [10] A. Nunnenkamp, K. Børkje, J. G. E. Harris, and S. M. Girvin, *Phys. Rev. A* **82**, 021806 (2010).
- [11] M. Asjad, G. S. Agarwal, M. S. Kim, P. Tombesi, G. Di Giuseppe, and D. Vitali, *Phys. Rev. A* **89**, 023849 (2014).
- [12] J. C. Sankey, C. Yang, B. M. Zwickl, A. M. Jayich, and J. G. E. Harris, *Nat. Phys.* **6**, 707 (2010).
- [13] T. K. Paraiso, M. Kalaei, L. Zang, H. Pfeifer, F. Marquardt, and O. Painter, *Phys. Rev. X* **5**, 041024 (2015).
- [14] H. Kaviani, C. Healey, M. Wu, R. Ghobadi, A. Hryciw, and P. E. Barclay, *Optica* **2**, 271 (2015).
- [15] C. Doolin, B. D. Hauer, P. H. Kim, A. J. R. MacDonald, H. Ramp, and J. P. Davis, *Phys. Rev. A* **89**, 053838 (2014).
- [16] G. A. Brawley, M. R. Vanner, P. E. Larsen, S. Schmid, A. Boisen, and W. P. Bowen, *Nat. Commun.* **7**, 10988 (2016).
- [17] H. Miao, S. Danilishin, T. Corbitt, and Y. Chen, *Phys. Rev. Lett.* **103**, 100402 (2009).
- [18] F. Elste, S. M. Girvin, and A. A. Clerk, *Phys. Rev. Lett.* **102**, 207209 (2009).
- [19] J. M. Dobrindt and T. J. Kippenberg, *Phys. Rev. Lett.* **104**, 033901 (2010).
- [20] K. Jacobs, L. Tian, and J. Finn, *Phys. Rev. Lett.* **102**, 057208 (2009).
- [21] M. R. Vanner, *Phys. Rev. X* **1**, 021011 (2011).
- [22] H. K. Cheung and C. K. Law, *Phys. Rev. A* **84**, 023812 (2011).
- [23] A. Xuereb and P. Domokos, *New J. Phys.* **14**, 095027 (2012).
- [24] C. W. Gardiner and P. Zoller, *Quantum Noise* (Springer, Berlin, 2004).
- [25] A. A. Clerk, M. H. Devoret, S. M. Girvin, F. Marquardt, and R. J. Schoelkopf, *Rev. Mod. Phys.* **82**, 1155 (2010).
- [26] A. Xuereb, R. Schnabel, and K. Hammerer, *Phys. Rev. Lett.* **107**, 213604 (2011).
- [27] A. Sawadsky, H. Kaufer, R. M. Nia, S. P. Tarabrin, F. Y. Khalili, K. Hammerer, and R. Schnabel, *Phys. Rev. Lett.* **114**, 043601 (2015).
- [28] C. Reinhardt, T. Müller, A. Bourassa, and J. C. Sankey, *Phys. Rev. X* **6**, 021001 (2016).
- [29] F. Marquardt, J. P. Chen, A. A. Clerk, and S. M. Girvin, *Phys. Rev. Lett.* **99**, 093902 (2007).
- [30] F. Marquardt, A. A. Clerk, and S. M. Girvin, *J. Mod. Opt.* **55**, 3329 (2008).
- [31] T. Caniard, P. Verlot, T. Briant, P. F. Cohadon, and A. Heidmann, *Phys. Rev. Lett.* **99**, 110801 (2007).
- [32] U. Fano, *Phys. Rev.* **124**, 1866 (1961).
- [33] A. E. Miroshnichenko, S. Flach, and Y. S. Kivshar, *Rev. Mod. Phys.* **82**, 2257 (2010).
- [34] T. Weiss, C. Bruder, and A. Nunnenkamp, *New J. Phys.* **15**, 045017 (2013).
- [35] T. Weiss and A. Nunnenkamp, *Phys. Rev. A* **88**, 023850 (2013).
- [36] F. Y. Khalili, S. P. Tarabrin, R. Schnabel, and K. Hammerer, [arXiv:1604.01309](https://arxiv.org/abs/1604.01309).